Evidence for dynein and astral microtubule–mediated cortical release and transport of $G\alpha_i$/LGN/NuMA complex in mitotic cells

Zhen Zheng[a], Qingwen Wan[a], Jing Liu[b], Huabin Zhu[a], Xiaogang Chu[a], and Quansheng Du[a]
[a]Institute of Molecular Medicine and Genetics, Department of Neurology, Medical College of Georgia, Georgia Regents University, Augusta, GA 30912; [b]Ministry of Education Laboratory of Combinatorial Biosynthesis and Drug Discovery, Wuhan University School of Pharmaceutical Science, Wuhan 430072, China

ABSTRACT **Spindle positioning is believed to be governed by the interaction between astral microtubules and the cell cortex and involve cortically anchored motor protein dynein. How dynein is recruited to and regulated at the cell cortex to generate forces on astral microtubules is not clear. Here we show that mammalian homologue of *Drosophila* Pins (Partner of Inscuteable) (LGN), a $G\alpha_i$-binding protein that is critical for spindle positioning in different systems, associates with cytoplasmic dynein heavy chain (DYNC1H1) in a $G\alpha_i$-regulated manner. LGN is required for the mitotic cortical localization of DYNC1H1, which, in turn, also modulates the cortical accumulation of LGN. Using fluorescence recovery after photobleaching analysis, we show that cortical LGN is dynamic and the turnover of LGN relies, at least partially, on astral microtubules and DYNC1H1. We provide evidence for dynein- and astral microtubule–mediated transport of $G\alpha_i$/LGN/nuclear mitotic apparatus (NuMA) complex from cell cortex to spindle poles and show that actin filaments counteract such transport by maintaining $G\alpha_i$/LGN/NuMA and dynein at the cell cortex. Our results indicate that astral microtubules are required for establishing bipolar, symmetrical cortical LGN distribution during metaphase. We propose that regulated cortical release and transport of LGN complex along astral microtubules may contribute to spindle positioning in mammalian cells.**

Monitoring Editor
Xueliang Zhu
Chinese Academy of Sciences

Received: Jun 14, 2012
Revised: Jan 22, 2013
Accepted: Jan 30, 2013

INTRODUCTION

Mitotic spindle orientation plays a critical role during tissue morphogenesis by regulating organ size and shape. It is also the foundation for asymmetric cell division, a key step for stem cells to function in generating cellular diversity (Gonczy, 2008; Knoblich, 2008; Siller and Doe, 2009; Gillies and Cabernard, 2011; Morin and Bellaiche, 2011).

During the asymmetric cell division of *Drosophila* neuroblasts and sensory organ precursor cells, the reorientation of mitotic spindle has been shown to require a protein called Partner of Inscuteable (Pins) and the Gα subunit of the heterotrimeric G proteins, which localize asymmetrically at the cell cortex during mitosis (Parmentier *et al.*, 2000; Schaefer *et al.*, 2000, 2001; Fuse *et al.*, 2003; Yu *et al.*, 2006; Chia *et al.*, 2008). Gene products related to Pins (GPR1/2) and Gα are also essential for spindle positioning and displacement during asymmetric cell division of the *Caenorhabditis elegans* zygotes (Gotta and Ahringer, 2001; Gotta *et al.*, 2003; Colombo *et al.*, 2003; Srinivasan *et al.*, 2003). Elegant laser cutting experiments and living-embryo time-lapse analysis suggest that GPR 1/2 and Gα subunits are required for generating unequal pulling forces on the mitotic apparatus (Grill *et al.*, 2001, 2003; Grill and Hyman, 2005; Pecreaux *et al.*, 2006).

We showed previously that mammalian homologue of *Drosophila* Pins (LGN) functions as a conformational switch that links $G\alpha_i$ and the nuclear mitotic apparatus (NuMA) protein and that LGN and $G\alpha_i$ may exert forces on mitotic spindles in cultured mammalian cells (Du *et al.*, 2001, 2002; Du and Macara, 2004). Subsequent studies identified Mud from *Drosophila* and Lin5 in *C. elegans* as functional homologues of NuMA (Bowman *et al.*,

This article was published online ahead of print in MBoC in Press (http://www.molbiolcell.org/cgi/doi/10.1091/mbc.E12-06-0458) on February 6, 2013.

Address correspondence to: Quansheng Du (qdu@gru.edu).

Abbreviations used: DYNC1H1, dynein heavy chain, cytoplasmic 1; DYNC1I1, dynein IC 1; FRAP, fluorescence recovery after photobleaching; LatA, latrunculin A; LGN, mammalian homologue of *Drosophila* Partner of Inscuteable; MT, microtubule; NuMA, nuclear mitotic apparatus.

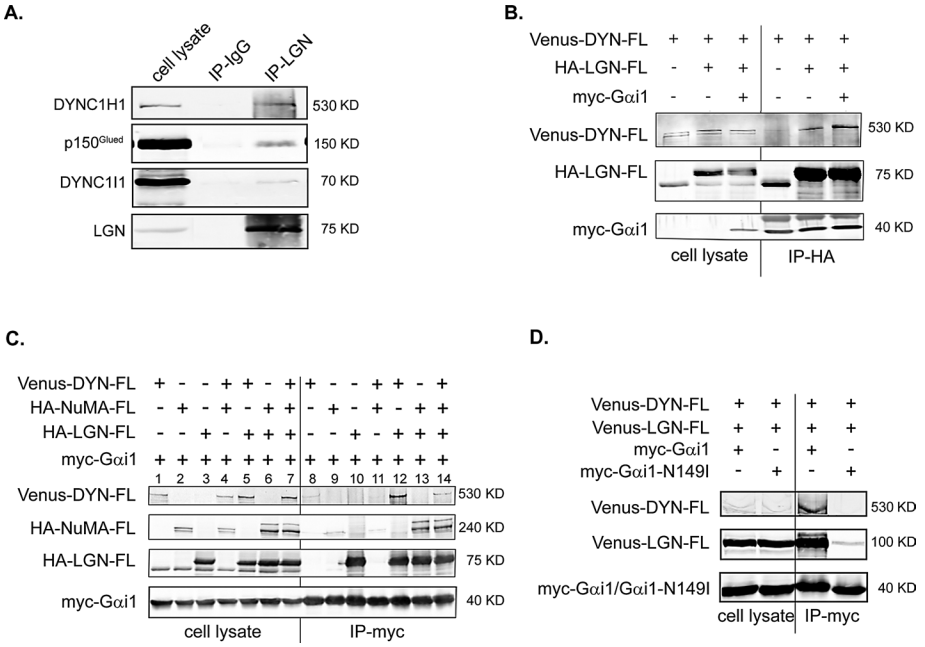

FIGURE 1: $G\alpha_i$-regulated interaction between LGN and DYNC1H1. (A) Endogenous LGN and cytoplasmic dynein form a complex. MDCK II cells were partially synchronized by treating with nocodazole (200 nM) for 12 h. After being released from the treatment for 40 min, cells were harvested and subjected to immunoprecipitation using anti-LGN antibodies or rabbit IgG. The immunoprecipitates were separated by SDS–PAGE and blotted using specific antibodies. (B) $G\alpha_i$ enhances the association between LGN and DYNC1H1. Cos 7 cells were transfected as indicated. Cell lysates (1/30 of total) and immunoprecipitates were separated in a 6% SDS–PAGE gel and blotted using specific antibodies. Note that in 6% gel, myc-$G\alpha_i$1 comigrated with and was masked by the light chain of anti-HA antibody in the HA-LGN immunoprecipitates. (C) $G\alpha_i$, LGN, and DYNC1H1 form a complex in vivo, independent of NuMA. Cos 7 cells were transfected as indicated. Cell lysates (1/30 of total) and immunoprecipitates were separated in a 7% SDS–PAGE gel and blotted. (D) The GoLoco-insensitive $G\alpha_i$1 cannot associate with LGN and DYNC1H1. Cos 7 cells were transfected as indicated. Cell lysates were subjected to analysis as in C.

2006; Izumi *et al.*, 2006; Siller *et al.*, 2006; van der Voet *et al.*, 2009), suggesting the existence of an evolutionarily conserved protein complex in regulating spindle positioning. The in vivo function of mammalian $G\alpha_i$/LGN/NuMA complex was not clear until recently. Accumulating evidence suggest that this ternary complex plays an important role in directing spindle orientation, not only in asymmetrically dividing stem/progenitor cells during development, but also in symmetrically dividing cells during epithelial morphogenesis (Morin *et al.*, 2007; Konno *et al.*, 2008; Hao *et al.*, 2010; Poulson and Lechler, 2010; Zheng *et al.*, 2010; Ben-Yair *et al.*, 2011; El-Hashash and Warburton, 2011; El-Hashash *et al.*, 2011; Peyre *et al.*, 2011; Williams *et al.*, 2011; Zhu *et al.*, 2011; Matsumura *et al.*, 2012; Xiao *et al.*, 2012).

Spindle positioning is believed to be regulated by the interaction between astral microtubules (MTs) and the cell cortex (McCarthy and Goldstein, 2006). How the cortical Gα/LGN/NuMA ternary complex is physically linked to astral MTs is not completely understood. Although NuMA can bind to MTs, it cannot do so when associated with LGN (Du *et al.*, 2002; Gaetz and Kapoor, 2004; Kisurina-Evgenieva *et al.*, 2004). Another plausible candidate is cytoplasmic dynein, the most abundant minus end–directed, microtubule-based motor protein complex (Kardon and Vale, 2009). Studies from different systems suggest that cytoplasmic dynein and its functionally linked dynactin complex are involved in orienting mitotic spindles (Carminati and Stearns, 1997; Adames and Cooper, 2000; O'Connell and Wang, 2000; Dujardin and Vallee, 2002; Ahringer, 2003). The relationship between dynein and the Pins family of proteins is evident in asymmetrically dividing *C. elegans* zygotes, in which GPR-1/2 and Gα are linked to subunits of the dynein/dynactin complex in generating pulling forces on astral MTs (Grill *et al.*, 2001, 2003; Pecreaux *et al.*, 2006; Couwenbergs *et al.*, 2007; Nguyen-Ngoc *et al.*, 2007). More recently, the link between the ternary complex and cytoplasmic dynein was also established in mitotic HeLa cells (Toyoshima *et al.*, 2007; Woodard *et al.*, 2010; Kiyomitsu and Cheeseman, 2012). However, it is not clear which component of the ternary complex mediates the association with cytoplasmic dynein and how the association is regulated.

The current view of dynein-mediated force generation on astral MTs is that dynein is anchored at the cell cortex and interacts with astral MTs (Grill and Hyman, 2005; Hendricks *et al.*, 2012; Laan *et al.*, 2012). How dynein is anchored and regulated at the cell cortex is not known. Furthermore, dynein was also observed to localize along astral MTs (Busson *et al.*, 1998), and in principle, dynein movement along astral MTs can also produce pulling forces (Kimura and Kimura, 2011), although such evidence is missing in mitotic mammalian cells. Recent studies also suggest that cortical actin filaments are involved in spindle positioning, either intrinsically or in response to external cues (Thery *et al.*, 2005; Toyoshima and Nishida, 2007; Kunda and Baum, 2009; Fink *et al.*, 2011). Whether and how actin filaments are linked to dynein-based force generator are not clear.

Here we show that LGN and cytoplasmic dynein heavy chain form a complex and regulate each other for their cortical localization and that actin filaments help to maintain LGN/dynein at the cell cortex and counteract astral microtubule–mediated cortical release and transport of LGN/dynein complex.

RESULTS

$G\alpha_i$-regulated association of LGN and dynein heavy chain, cytoplasmic 1 in mammalian cells

To test whether LGN associates with the dynein/dynactin complex in mammalian cells, we performed immunoprecipitation analysis using Madin–Darby canine kidney (MDCK) cells that were partially synchronized in mitosis. As shown in Figure 1A, anti-LGN antibodies, but not rabbit immunoglobulin G (IgG), could efficiently immunoprecipitate endogenous dynein heavy chain, cytoplasmic 1 (DYNC1H1). Small but specific amounts of dynein IC 1 (DYNC1I1) and dynactin subunit $p150^{Glued}$ were also detected in the anti-LGN immunoprecipitates, indicating that endogenous LGN and cytoplasmic dynein form a complex. Our results are consistent with a recent study showing that ectopically expressed green fluorescent protein (GFP)–LGN forms a complex with cytoplasmic dynein in HeLa cells (Kiyomitsu and Cheeseman, 2012).

Because DYNC1H1 turned out to be the major coimmunoprecipitate of LGN, we further studied the interaction between LGN and DYNC1H1 by coexpressing full-length DYNC1H1 and LGN in

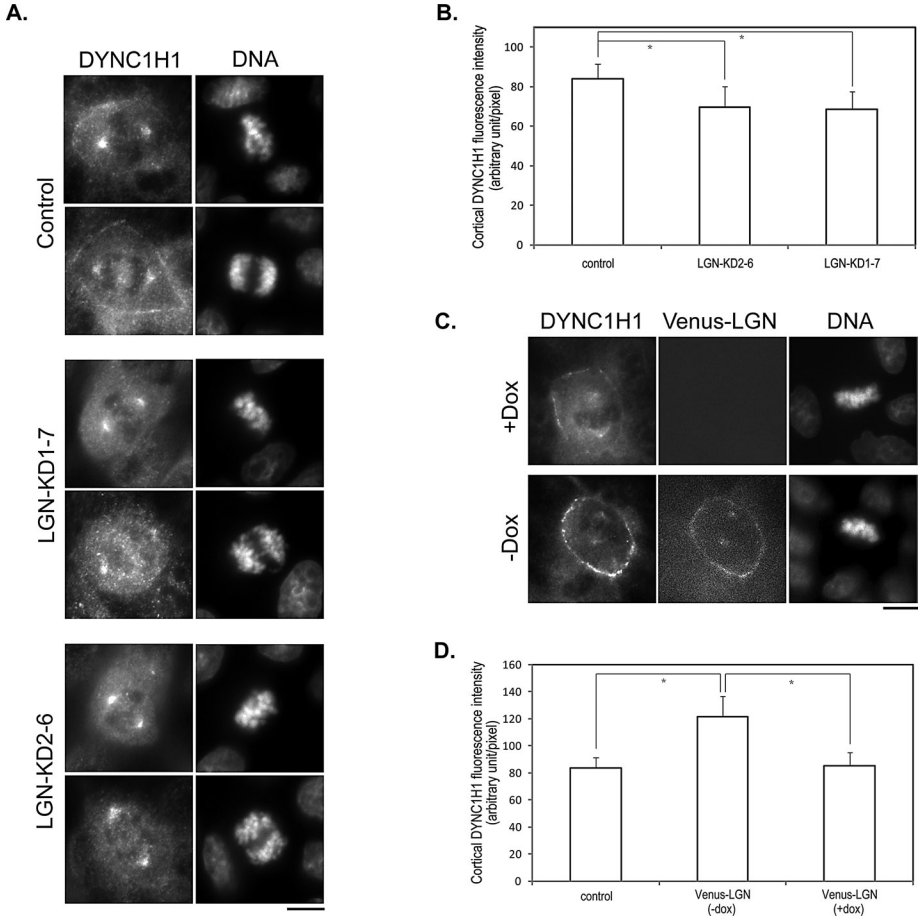

FIGURE 2: LGN is required for the cortical localization of DYNC1H1 during mitosis. (A) LGN depletion results in reduced cortical localization of DYNC1H1. MDCK cells transduced by control lentivirus (control) or lentivirus expressing shRNAs targeting different regions of LGN (LGN-KD1-7 and LGN-KD2-6) were stained with anti-DYNC1H1 antibody and DNA dye. Bar, 10 μm. (B) Quantitation of the fluorescence intensity of cortical DYNC1H1 from images acquired in A. $n = 50$ for each set; $^*p < 0.01$. (C) Slight overexpression of LGN leads to enhanced cortical localization of DYNC1H1. Stable Tet-Off MDCK cells expressing Venus-LGN were cultured in the presence (+Dox) or absence (–Dox) of doxycycline. At 24 h later, cells were stained as in A. Bar, 10 μm. (D) Quantitation of the fluorescence intensity of cortical DYNC1H1 from images acquired in C. $n = 50$ for each set; $^*p < 0.01$.

Cos 7 cells. Immunoprecipitation of HA-LGN resulted in the coprecipitation of Venus-DYNC1H1 (Figure 1B), further suggesting that they can form a complex in vivo. The C-terminus of LGN contains four GoLoco motifs that bind to GDP-bound $G\alpha_{i/o}$ (Lanier, 2004; Willard *et al.*, 2004). LGN is normally in its closed conformation due to intramolecular interactions, and $G\alpha_i$ binding could switch LGN to an open state (Du and Macara, 2004). To test the effect of $G\alpha_i$ on the association between LGN and DYNC1H1, we included $G\alpha_i1$ in the cotransfection and immunoprecipitation experiments. Of interest, coexpression of myc-$G\alpha_i1$ led to obviously enhanced coimmunoprecipitation of Venus-DYNC1H1 with HA-LGN (Figure 1B), suggesting that the association between LGN and DYNC1H1 might rely on the conformation of LGN and could be regulated by $G\alpha_i1$ binding.

Next we tested whether DYNC1H1, LGN, and $G\alpha_i$ can form a complex in vivo by transfecting cells with different combinations of $G\alpha_i1$, LGN, and DYNC1H1. As shown in Figure 1C, myc-$G\alpha_i1$ could efficiently immunoprecipitate HA-LGN (lanes 3 and 10). In the absence of HA-LGN, myc-$G\alpha_i1$ could immunoprecipitate little, if any, Venus-DYNC1H1 (lanes 1 and 8). However, when HA-LGN was coexpressed, myc-$G\alpha_i1$ could efficiently immunoprecipitate Venus-DYNC1H1 (lanes 5 and 12), suggesting that $G\alpha_i1$, LGN, and DYNC1H1 can form a ternary complex in vivo.

We showed previously that NuMA can also bind to LGN and form a complex with LGN and $G\alpha_i$ (Du and Macara, 2004). NuMA was also shown to associate with dynein/dynactin complex in *Xenopus* egg extracts (Merdes *et al.*, 1996). It is possible that endogenous NuMA is mediating the association between $G\alpha_i$/LGN and DYNC1H1. To test the effect of NuMA on the DYNC1H1/LGN/$G\alpha_i$ complex formation, we included NuMA in the cotransfection experiments. Whereas myc-$G\alpha_i1$ can immunoprecipitate HA-NuMA in the presence of HA-LGN (Figure 1C, lanes 6 and 13), coexpression of HA-NuMA resulted in reduced Venus-DYNC1H1 in the myc-$G\alpha_i1$/HA-LGN complex (lanes 7 and 14), suggesting that $G\alpha_i1$/LGN/DYNC1H1 complex formation is unlikely to be mediated through NuMA.

To exclude the possibility that the association between DYNC1H1 and $G\alpha_i1$ is mediated through other $G\alpha_i1$-binding proteins such as $G\beta/\gamma$ (Sachdev *et al.*, 2007), we used a GoLoco-insensitive $G\alpha_i$ mutant ($G\alpha_i1$-N149I) as a control. This mutant $G\alpha_i1$ specifically lacks the ability to bind to the GoLoco motif but is otherwise equivalent to wild-type $G\alpha_i1$ in terms of other functional aspects, including binding to G β/γ subunits (Willard *et al.*, 2008). As shown in Figure 1D, whereas wild-type $G\alpha_i1$ could efficiently immunoprecipitate LGN and DYNC1H1, the GoLoco-insensitive $G\alpha_i1$ mutant failed to do so, suggesting that the $G\alpha_i1$/DYNC1H1 complex formation is mediated through LGN.

LGN is necessary and sufficient for the cortical localization of DYNC1H1 during mitosis

The interaction between LGN and DYNC1H1 prompted us to test whether LGN is required for the cortical localization of DYNC1H1. Cortical localization of dynactin subunits in MDCK cells had been described (Busson *et al.*, 1998; Faulkner *et al.*, 2000). Using an antibody against DYNC1H1, we could detect both spindle and cortical localization of DYNC1H1 (Figure 2A). The authenticity of the antibody staining was verified by using two different short hairpin RNAs (shRNAs) against canine DYNC1H1, which, upon expression, significantly eliminated the cortical and spindle staining of DYNC1H1 (Supplemental Figure S1). We then compared DYNC1H1 staining between control and stable LGN knockdown cells that we established previously (Zheng *et al.*, 2010). Remarkably, depletion of LGN led to significantly reduced cortical localization of DYNC1H1, whereas the spindle localization of DYNC1H1 appeared normal (Figure 2, A and B). These results are consistent with recent studies in HeLa cells showing that LGN is required for mitotic cortical localization of dynein/dynactin subunits (Woodard *et al.*, 2010; Kiyomitsu and Cheeseman, 2012).

We had established inducible MDCK cell lines that slightly overexpress Venus-tagged LGN (Du and Macara, 2004). Slight overexpression of LGN led to enhanced cortical localization of LGN and profound spindle oscillation, suggesting unbalanced forces on astral MTs (Du and Macara, 2004). We used these cell lines to test the effect of LGN overexpression on DYNC1H1 localization during mitosis. Of interest, slight overexpression of Venus-LGN resulted in significantly enhanced cortical localization of DYNC1H1 (Figure 2, C and D). These data suggest that LGN is capable of recruiting DYNC1H1 to the cell cortex during mitosis, and, most important, endogenous LGN is required for the cortical localization of DYNC1H1 during mitosis.

Dynein and astral MTs regulate the cortical localization of LGN

Surprisingly, when we compared the localization of endogenous LGN in control and DYNC1H1-knockdown cells, we found that the cortical localization of LGN was obviously enhanced in DYNC1H1-knockdown cells (Figure 3, A and C), suggesting that DYNC1H1 also regulates LGN localization. As the minus end–directed motor protein, cortical dynein is believed to exert its function through astral MTs. We wondered whether disrupting astral MTs would also affect LGN distribution. We treated cells with low doses of nocodazole, which is generally used to disrupt astral MTs (Jordan *et al.*, 1992). Indeed, treating MDCK cells with 50 nM nocodazole led to significant loss of astral MTs, whereas the spindle MTs were not affected (Supplemental Figure S2). Of interest, disruption of astral MTs also led to enhanced cortical localization of LGN (Figure 3, B and C). Thus, whereas LGN is required for the cortical recruitment of dynein, dynein also regulates cortical LGN through astral MTs.

Dynein- and astral MT–dependent turnover of cortical LGN

The fact that cortical LGN is modulated by dynein and astral MTs led us to speculate that it might be dynamic. We performed fluorescence recovery after photobleaching (FRAP) experiments to study the kinetics of cortical LGN using our Venus-LGN cell line. As we showed previously (Du and Macara, 2004), in live MDCK cells, cortical Venus-LGN usually exhibits a patchy distribution (Figure 4A), which is consistent with a recent report showing that GFP-DYNC1H1 also shows patchy localization at the cell cortex (Collins *et al.*, 2012). Our FRAP analysis indicated that; indeed the fluorescence of cortical Venus-LGN recovered gradually after photobleaching, suggesting dynamic turnover (Figure 4 and Supplemental Movie S1). Next we set out to test whether astral MTs and DYNC1H1 are involved in the dynamic turnover of cortical LGN. We carried out similar FRAP experiments under conditions when astral MTs were disrupted using low doses of nocodazole or DYNC1H1 was knocked down by specific shRNA. Of interest, the fluorescence recovery of cortical Venus-LGN was significantly inhibited under both conditions (Figure 4, A–E, and Supplemental Movies S2 and S3), suggesting that astral MTs and DYNC1H1 contribute to the dynamic turnover of cortical LGN.

It is possible that astral MTs and dynein-dependent turnover of cortical LGN are mediated through the dissociation of LGN from the dynein complex into cytosol when astral MTs reach the cell cortex. Alternatively, LGN might be transported by dynein along astral MTs. To distinguish these possibilities, we asked whether we could detect LGN on astral MTs. Indeed, in Venus-LGN cells, we observed LGN localization along astral MTs by using either the anti-LGN antibody (Figure 4F) or the anti-GFP antibody (unpublished data). Of note, Venus-LGN was not observed to localize on spindle MTs.

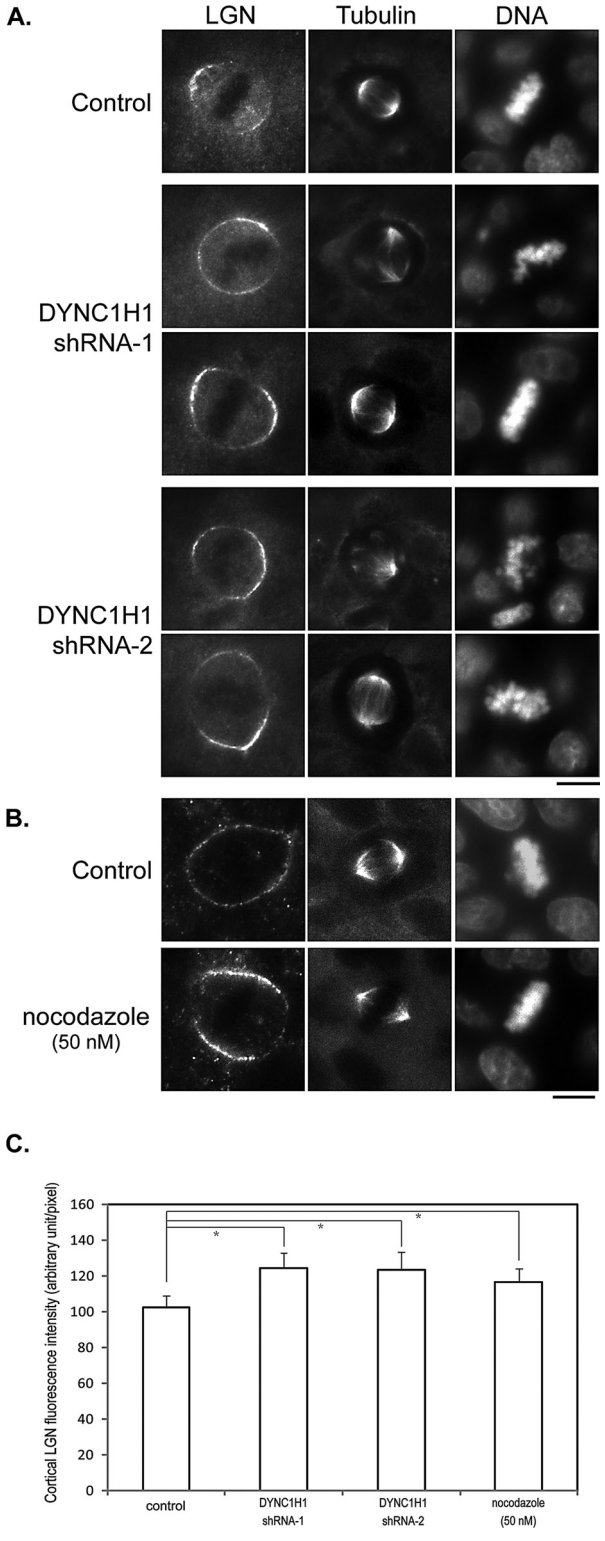

FIGURE 3: Knocking down DYNC1H1 or disrupting astral MTs leads to enhanced cortical localization of LGN. (A) MDCK cells were transfected with plasmids expressing control shRNA (control) or shRNAs targeting DYNC1H1 (shRNA1 and shRNA2). At 48 h later, cells were fixed and stained with anti-LGN, anti–α-tubulin antibodies, and DNA dye. Bar, 10 μm. (B) MDCK cells were cultured in media containing 50 nM nocodazole for 40 min. Cells were then fixed and stained as in A. Bar, 10 μm. (C) Quantitation of the fluorescence intensity of cortical LGN from images acquired in A and B. $n = 50$ for each set; $^*p < 0.01$.

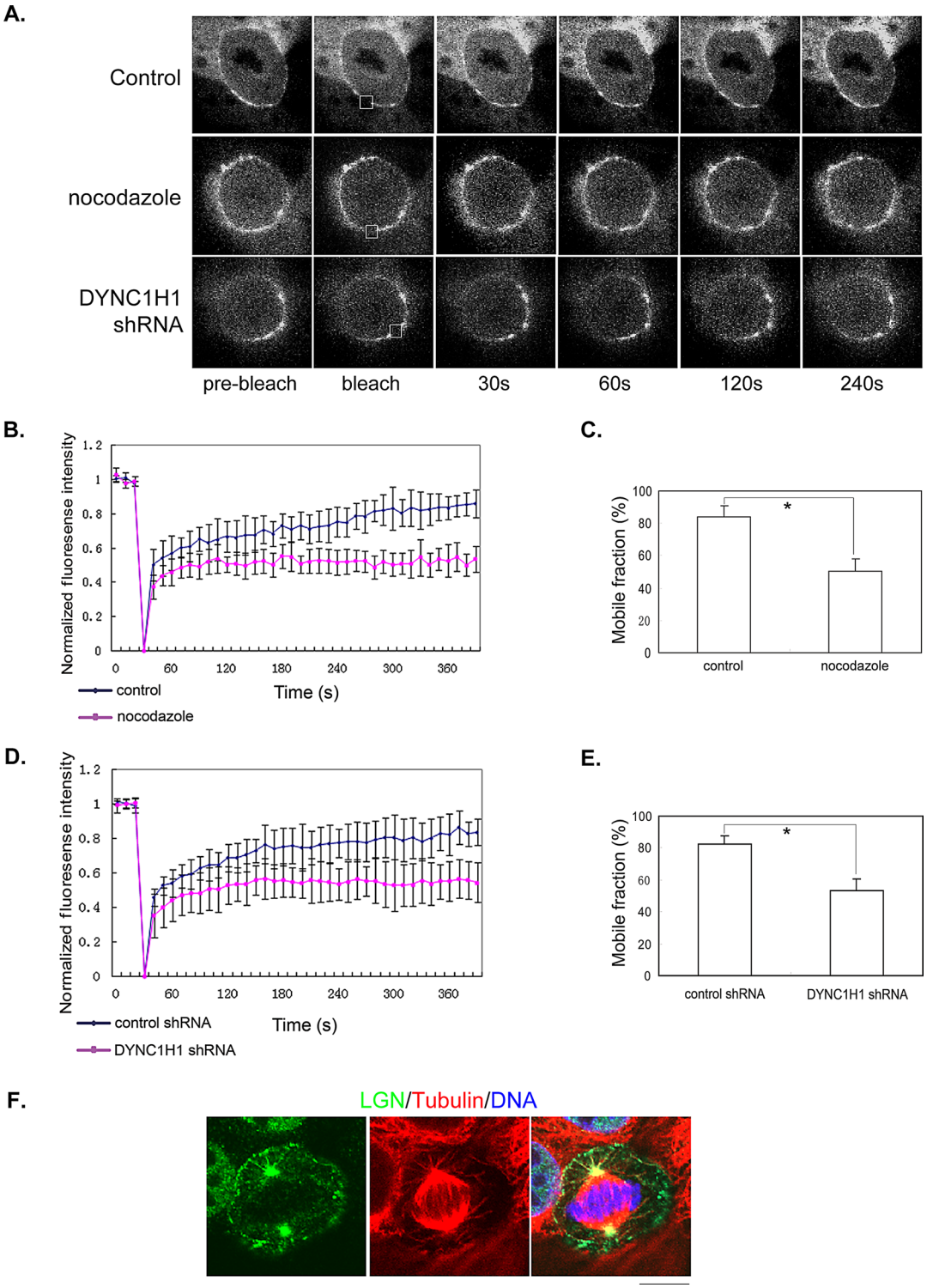

FIGURE 4: Dynamic turnover of cortical LGN relies on astral MTs and DYNC1H1. (A) FRAP analysis of cortical LGN. Representative images from live-cell time-lapse series were shown. The photobleaching areas were marked by squares. Stable MDCK cells expressing Venus-LGN were either untreated (top), treated with 50 nM nocodazole for 1 h (middle), or transfected with DYNC1H1 shRNA for 48 h (bottom) before being subjected to FRAP analysis. (B–E) Quantitative analysis of FRAP experiments. (B, D) Plots of normalized fluorescence intensity of cortical Venus-LGN in cells treated with DMSO (B, blue diamonds), 50 nM nocodazole (B, pink squares), or transfected with control shRNA (D, blue diamonds) or DYNC1H1 shRNA (D, pink squares) vs. time (in seconds) after photobleaching. Data are expressed as mean ±SEM ($n = 8$ for each set). (C, E) The mobile fractions of cortical Venus-LGN in control, nocodazole-treated, or DYNC1H1-knockdown cells were calculated from the fluorescence recovery curves shown in B and D. Data are expressed as mean ±SEM. *$p < 0.01$. (F) Association of Venus-LGN with astral MTs. MDCK cells expressing Venus-LGN were preextracted with microtubule stabilization buffer containing 0.2% Triton X-100 and then fixed with 4% PFA. Fixed cells were stained with anti-LGN (green), anti–α-tubulin (red) antibodies, and DNA dye (blue). Bar, 10 μm.

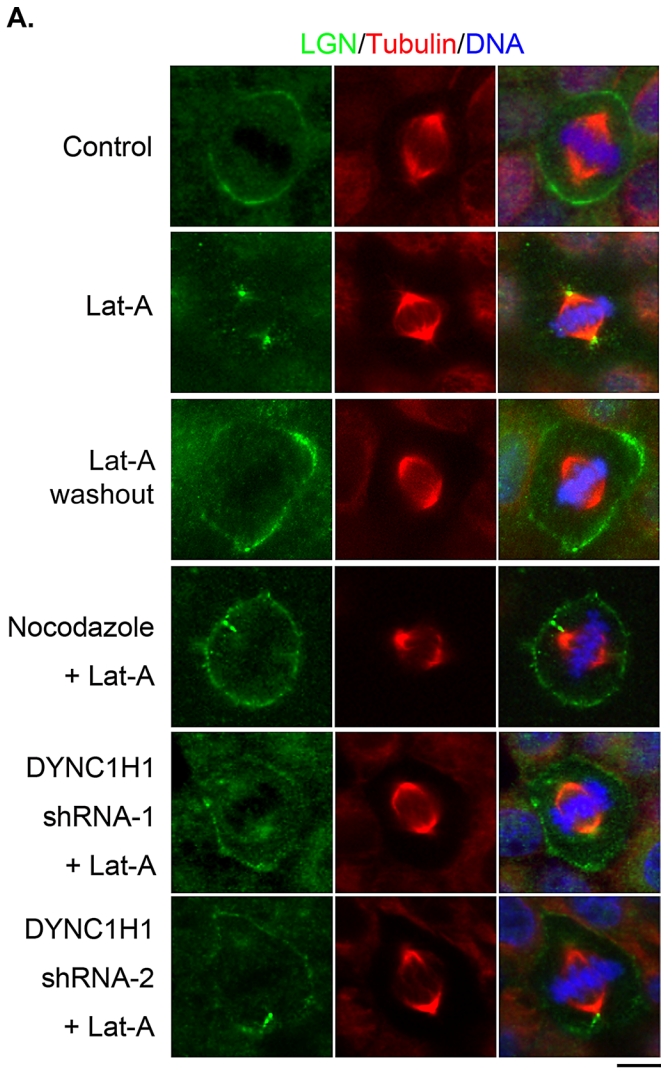

FIGURE 5: Disruption of actin filaments leads to astral microtubule– and dynein-dependent cortical dissociation and spindle pole accumulation of LGN. (A) MDCK II cells were either untreated (Control) or treated as labeled. LatA: 1 μM of LatA for 45 min; Nocodazole + LatA: 50 nM of nocodazole plus 1 μM of LatA for 45 min; DYNC1H1 shRNA-1, -2 + LatA: transfected with DYNC1H1 shRNA-1 or -2 for 48 h and then treated with 1 μM LatA for 45 min. MG132, 5 μM, was added 1 h before treatments and maintained during treatments. Cells were fixed after treatments and stained with anti-LGN (green), anti–α-tubulin (red) antibodies, and DNA dye (blue). (B) Quantitation of LGN signals at spindle poles as described in *Materials and Methods*. $n = 50$ for each set; $^*p < 0.01$.

Dynein and astral MTs mediate transport of LGN from cell cortex to spindle poles

The cortical localization of LGN and dynein appears to rely on actin filaments (Busson *et al.*, 1998; Kaushik *et al.*, 2003; Toyoshima *et al.*, 2007), although the underlying mechanism is not known. Indeed, LGN dissociated from the cell cortex during mitosis when MDCK cells were treated with latrunculin A (LatA; Figure 5A), a drug that depolymerizes actin filaments (Spector *et al.*, 1983; Supplemental Figure S3). Consistent with previous studies in HeLa cells (Toyoshima and Nishida, 2007), disruption of actin filaments led to spindle misorientation in MDCK cells, although the overall spindle organization appeared normal (unpublished data). Of interest, although we could hardly detect spindle pole localization of endogenous LGN in untreated MDCK cells, we observed an obvious accumulation of LGN at the spindle poles in cells treated with LatA (Figure 5, A and B, and Supplemental Figure S3A). Of importance, the spindle pole accumulation of the anti-LGN staining was not observed in LGN-stable knockdown cells treated with LatA (Supplemental Figure S3B), indicating that it was endogenous LGN that translocated to the spindle poles when actin filaments were disrupted. Furthermore, after we washed out LatA from the cells, LGN regained cortical localization and disappeared from the spindle poles (Figure 5A). Similar results were observed when cells were treated with cytochalasin D, another inhibitor of actin filaments (unpublished data).

The aforementioned observations—cortical LGN underwent astral MTs and dynein-dependent turnover, and LGN was detected along astral MTs (Figure 4)—led us to wonder whether LatA-induced cortical dissociation and spindle pole accumulation of LGN are mediated through an active transport process that involved astral MTs and dynein. If so, we would expect that blocking such transport might attenuate the effect of LatA on LGN. To test this hypothesis, we included low doses of nocodazole in the LatA treatment. Strikingly, the presence of nocodazole significantly preserved the cortical localization of LGN and inhibited the spindle pole accumulation of LGN (Figure 5, A and B). It is noteworthy that nocodazole-mediated preservation of cortical LGN was not due to incomplete disruption of actin filaments (Supplemental Figure S3A). Similar results were obtained when DYNC1H1-knockdown cells were treated with LatA (Figure 5, A and B), suggesting that the translocation of LGN after LatA treatment requires astral MTs and cytoplasmic dynein. To explore whether such phenomena are specific to adherent, polarized epithelial cells, we performed identical experiments in MDA-231 and HeLa cells and observed similar results (Supplemental Figure S4 and unpublished data).

Astral MTs mediate release and transport of cortical dynein and NuMA when actin filaments are disrupted

We showed that LGN forms a complex with DYNC1H1 and is required for the cortical localization of DYNC1H1 (Figures 1 and 2). If LGN is transported by cortical dynein, we would expect dissociation of DYNC1H1 from the cortex when cells were treated with LatA. We used our Venus-LGN cell line to investigate the distribution of DYNC1H1, as more robust cortical staining of DYNC1H1 was observed in these cells (Figure 2C). As shown in Figure 6A (second from top), LatA treatment led to diminished cortical localization of Venus-LGN and endogenous

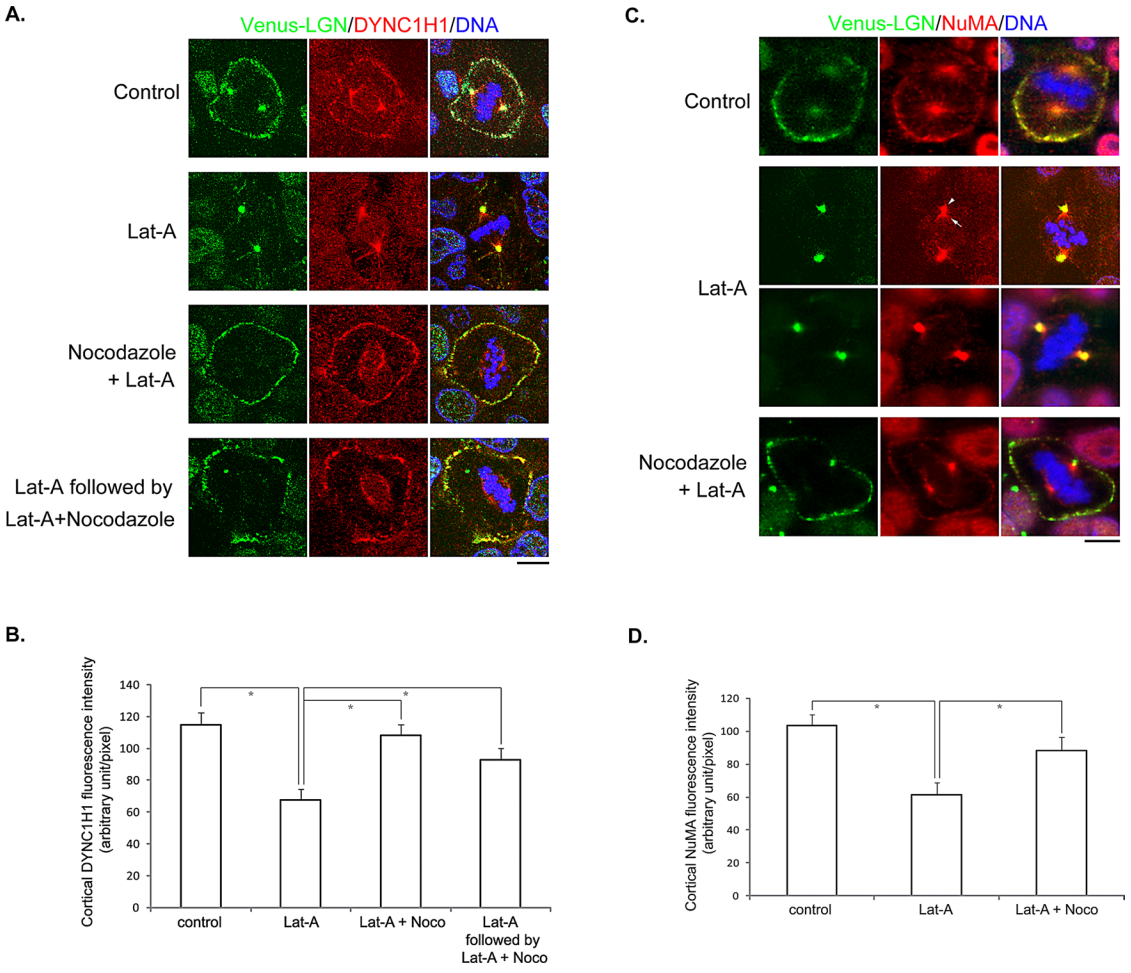

FIGURE 6: Disruption of actin filaments leads to astral microtubule–dependent cortical dissociation and spindle pole accumulation of DYNC1H1 and NuMA. (A) Venus-LGN–expressing cells were treated as in Figure 5A except for the results at the bottom, for which cells were first treated with 1 μM LatA for 45 min and then treated with 1 μM LatA plus 50 nM nocodazole for another 45 min. Cells were stained with anti-DYNC1H1 antibody (red) and DNA dye (blue). (B) Quantitation of cortical DYNC1H1 fluorescence intensity as described in *Materials and Methods*. $n = 50$ for each set; $^*p < 0.01$. (C) Venus-LGN–expressing cells were treated as in A. Cells were stained with anti-NuMA antibody (red) and DNA dye (blue). Second from top, arrow points to the original crescent-shaped NuMA, and arrowhead points to NuMA accumulated at the spindle pole. (D) Quantitation of cortical NuMA fluorescence intensity. $n = 50$ for each set; $^*p < 0.01$. Bars, 10 μm.

DYNC1H1. We also observed more Venus-LGN and DYNC1H1 accumulating at the spindle poles (Figure 6A, second from top). Intriguingly, including low doses of nocodazole prevented LatA-induced cortical dissociation and spindle pole accumulation of Venus-LGN and DYNC1H1 (Figure 6, A, second from bottom, and B), further suggesting that dynein-mediated transport of LGN underlies the observed translocation of LGN upon disruption of actin filaments. These results also suggest that the cortical targeting of LGN/DYNC1H1 complex may not require actin filaments. It is still possible, however, that actin filaments are required for the initial cortical targeting of LGN/DYNC1H1 complex before the LatA plus nocodazole treatment. To clarify this issue, we pretreated cells with LatA to dissociate LGN/DYNC1H1 complex from the cell cortex and then added low doses of nocodazole while maintaining same amount of LatA in the medium. Such treatments resulted in significant relocalization of Venus-LGN and DYNC1H1 to the cell cortex (Figure 6, A, bottom, and B). Live-cell analysis also revealed LatA-induced cortical dissociation and spindle pole accumulation of Venus-LGN and the rescue effect of nocodazole in the presence of LatA (Supplemental Figure S5). These results indicate that LGN-mediated cortical targeting of dynein does not require actin filaments, and actin filaments may serve to maintain LGN/dynein at the cell cortex during mitosis.

Next we tested whether NuMA also follows a similar pattern as LGN and dynein. In untreated Venus-LGN cells, in addition to the well-known crescent-shaped structure near the spindle poles, endogenous NuMA was also observed at the cell cortex and along astral MTs (Figure 6C, top). After LatA treatment, NuMA dissociated from the cell cortex and was often seen to accumulate and colocalize with Venus-LGN at the spindle poles (Figure 6, C, middle, arrowhead, and D) adjacent to the original crescent (Figure 6C, middle, arrow). Disrupting astral MTs blocked LatA-induced dissociation of NuMA from the cell cortex (Figure 6, C, bottom, and D). Similar results were observed in MDA-231 cells (Supplemental Figure S4).

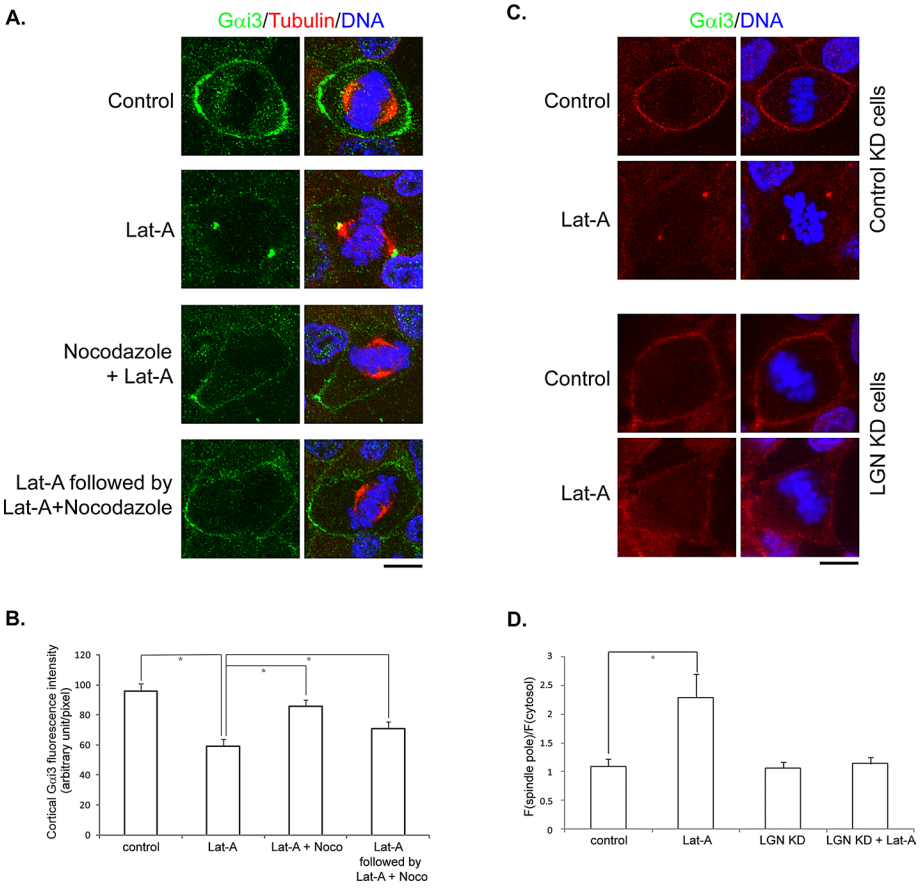

FIGURE 7: Disruption of actin filaments leads to astral microtubule– and LGN-dependent cortical release and spindle pole accumulation of $G\alpha_i3$. (A) MDCK II cells were treated as in Figure 5A. Cells were fixed after treatments and stained with anti-$G\alpha_i3$ (green), anti–α-tubulin (red) antibodies, and DNA dye (blue). (B) Quantitation of cortical $G\alpha_i3$ fluorescence intensity. $n = 50$ for each set; $^*p < 0.01$. (C) Stable MDCK cells expressing control shRNA (top two) or shRNA against LGN (bottom two) were either untreated (control) or treated with 1 μM of LatA for 45 min (LatA). Cells were fixed and stained with anti-$G\alpha_i3$ (red) and DNA dye (blue). (D) Quantitation of $G\alpha_i3$ signals at spindle poles as described in *Materials and Methods*. $n = 50$ for each set; $^*p < 0.01$.

Astral microtubule– and LGN-mediated transport of $G\alpha_i$

Because $G\alpha_i$ binds to LGN and regulates the association between LGN and DYNC1H1, we studied the effect of LatA treatment on the distribution of endogenous $G\alpha_i$. In untreated MDCK cells, $G\alpha_i3$ localized at the cell cortex in a similar pattern as LGN (Figure 7A). Of interest, LatA treatment resulted in significant cortical reduction and spindle pole accumulation of $G\alpha_i3$ (Figure 7, A and B), which is reminiscent of the effects of LatA on the distribution of LGN, DYNC1H1, and NuMA. Furthermore, the effect of LatA on the localization of $G\alpha_i3$ could be inhibited by low concentrations of nocodazole (Figure 7, A and B), suggesting that it was mediated by astral MTs. To test whether LatA-induced translocation of $G\alpha_i3$ was mediated through LGN, we compared control and LGN-knockdown cells. Consistent with previous work (Woodard *et al.*, 2010; Kiyomitsu and Cheeseman, 2012), knockdown of LGN did not obviously affect the membrane association of $G\alpha_i3$ in untreated cells (Figure 7, C and D). However, in the absence of LGN, LatA treatment did not lead to spindle pole accumulation of $G\alpha_i3$ (Figure 7, C and D). These results suggest that when actin filaments were disrupted, cortical $G\alpha_i3$ was also transported to the spindle poles along astral MTs through the LGN/dynein complex.

Astral microtubule–mediated transport is important for the establishment of bipolar, symmetrical cortical LGN distribution during metaphase

To maintain spindle positioning within a cell, cortical cues that exert forces on astral MTs need to be placed at confined regions of the cell cortex. Indeed, in metaphase HeLa cells, LGN is enriched at regions of the cell cortex that are close to the spindle poles, correlating perfectly with the spindle axis (Kiyomitsu and Cheeseman, 2012; Matsumura *et al.*, 2012). Recently a chromosome-associated Ran-GTP mechanism was proposed for excluding LGN from cortical regions near the spindle midzone (Kiyomitsu and Cheeseman, 2012). However, whether this mechanism can wholly account for the establishment of LGN distribution during metaphase is not clear. Our finding of dynein- and astral microtubule–mediated dynamic turnover of cortical LGN led us to test whether it is also involved in installing LGN at the cell cortex. We synchronized HeLa cells using thymidine block and arrested cells in mitosis with monastrol, an Eg5 kinesin inhibitor that prevents centrosome separation (Mayer *et al.*, 1999). In monastrol-arrested cells, LGN exhibited either diffused cortical localization or slight enrichment at one side of the cell cortex (Figure 8A, left). We then washed out monastrol and incubated cells in medium containing MG132, a proteasome inhibitor that prevents anaphase onset (Kisselev and Goldberg, 2001). One hour after monastrol washout, most of the mitotic cells had established bipolar spindles attached to properly aligned chromosomes (Figure 8A, middle). In these cells, LGN showed confined, bipolar and symmetrical distribution at cortical regions facing the spindle poles and was excluded from the central cell cortex (Figure 8A, middle), identical to its localization in untreated metaphase cells. Thus the monastrol washout experiments allowed us to study how the spatial arrangement of cortical LGN was achieved. To test whether astral MTs were involved, we included 20 nM nocodazole in the medium after monastrol washout. Of interest, such low concentration of nocodazole treatment led to LGN mislocalization in a large portion of cells with apparently normal chromosome alignment and bipolar spindle formation (Figure 8, A, right, and B), although the chromosome-mediated exclusion mechanism appeared to be working in most of the cases. These results suggest that astral MTs, and probably astral microtubule-mediated shuttling and subsequent recycling of cortical LGN, are required for establishing proper LGN distribution at the cell cortex.

DISCUSSION

Proper spindle positioning is believed to be achieved when astral MTs receive confined cortical forces (Grill and Hyman, 2005). The evolutionarily conserved Gα/LGN/NuMA ternary complex has emerged as an important cortical force generator (Gonczy, 2008; Knoblich, 2008; Siller and Doe, 2009), but how this complex exerts forces on astral MTs is not clear.

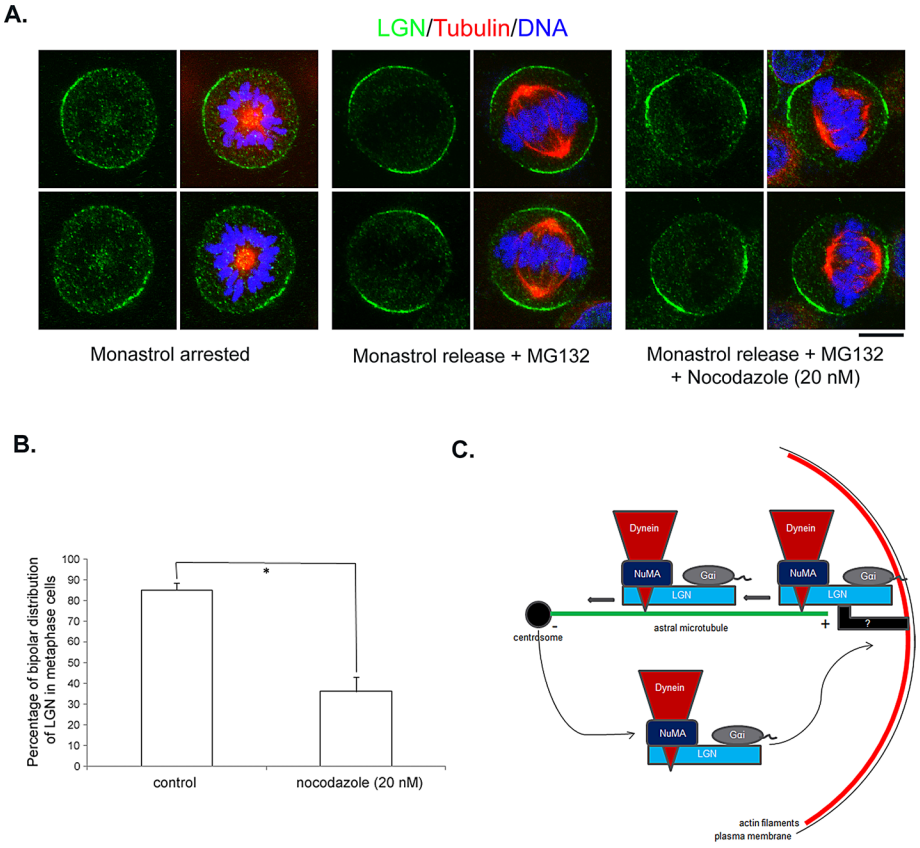

FIGURE 8: Astral MTs are required for establishing bipolar, symmetrical cortical LGN distribution during metaphase. (A) HeLa cells were partially synchronized by treating with 2 mM thymidine for 16 h. After release in normal medium for 8 h, cells were treated with 50 mM monastrol for 3 h. Monastrol-arrested cells were either directly fixed (left) or washed and released in normal medium containing 5 μM MG132 (middle) or 5 μM MG132 plus 20 nM nocodazole (right) for 1 h and fixed. Fixed cells were stained with anti-LGN (green), anti–α-tubulin (red) antibodies, and DNA dye (blue). Bar, 10 μm. (B) Quantitation of bipolar, symmetrical cortical LGN localization. Only cells with normal chromosome condensation and alignment were included in the quantification. $n = 100$ from three independent experiments; $^*p < 0.001$. (C) Schematic working model illustrating astral microtubule–mediated transport and recycling of the Gα/LGN/dynein/NuMA complex during mitosis.

Here we show that $G\alpha_i$, LGN, and DYNC1H1 form a complex in mammalian cells. Of interest, $G\alpha_i$ binding enhances the association between LGN and DYNC1H1, further supporting the conformation switch hypothesis for the Pins family of proteins (Du and Macara, 2004; Nipper *et al.*, 2007). It also suggests that regulators of $G\alpha_i$ may affect the interaction between LGN and DYNC1H1. Our results, together with recent studies in HeLa cells (Woodard *et al.*, 2010; Kiyomitsu and Cheeseman, 2012), indicate that LGN serves as a major cortical factor that recruits cytoplasmic dynein to the cell cortex during mitosis, probably through membrane-bound Gα. It is surprising that NuMA, the other LGN-binding partner, has an inhibitory effect on the association between $G\alpha_i$/LGN and DYNC1H1. NuMA was shown to associate with cytoplasmic dynein in *Xenopus* egg extracts (Merdes *et al.*, 1996). While the manuscript was under revision, Kotak *et al.* (2012) reported that the N-terminal of NuMA associates with cytoplasmic dynein, although a direct physical link with a specific dynein subunit is still missing. Our results suggest that $G\alpha_i$/LGN and DYNC1H1 might form a complex in a NuMA-independent manner. It is possible, however, that in our immunoprecipitation analysis, the overexpressed NuMA might sequester DYNC1H1 to a cellular compartment that is not accessible for the $G\alpha_i$/LGN complex. Nevertheless, we showed that NuMA also localizes to astral MTs and is transported to the spindle poles when actin filaments are disrupted, suggesting that it is in a complex with LGN and dynein. We propose that NuMA may associate with other component of the dynein/dynactin complex and function with LGN in recruiting or modulating dynein at the cell cortex during mitosis. Further studies are needed to determine whether the association between LGN and DYNC1H1 is direct or indirect and how the interaction is regulated by related proteins.

A prevalent view of dynein function in spindle positioning is that dynein is anchored at the cell cortex and exerts forces on astral MTs either by controlling microtubule dynamics or by driving microtubule sliding along the cell cortex (Grill and Hyman, 2005; Hendricks *et al.*, 2012; Laan *et al.*, 2012). We now provide evidence that cortical dynein may not be static; instead, it can be released and move, in complex with LGN and NuMA, along astral MTs. The movement of the dynein complex along astral MTs may generate pulling forces, as astral MTs could also be captured by other cortical microtubule-binding proteins rather than dynein (Samora *et al.*, 2011). Alternatively, the release and transport of dynein complex may provide a novel mechanism for mammalian cells to limit, balance, or terminate cortical dynein-generated pulling forces. Our results are consistent with a recent study in *C. elegans* suggesting that MTs regulate cortical localization of GPR-1/2 (Werts *et al.*, 2011). It would be interesting to test whether dynein-mediated transport of LGN could be applied to other systems.

An interesting phenomenon that has been observed in multiple mammalian cell lines is that, during metaphase, LGN exhibits bipolar, symmetrical cortical localization, which correlates nicely with spindle orientation, suggesting an intrinsic mechanism for spindle positioning. How is the confined LGN distribution established? Recently an elegant chromosome-mediated, cortical exclusion model was proposed (Kiyomitsu and Cheeseman, 2012), although the underlying mechanism is not clear. Here we show that astral MTs are also required for proper cortical LGN distribution, suggesting the involvement of multiple mechanisms. We propose that astral MT–mediated transport and recycling may help to sort and enrich LGN at cortical regions facing the spindle poles, where the interaction between astral MTs and the cell cortex should be more intensive.

It is intriguing to observe that when actin filaments were disrupted, endogenous $G\alpha_i$ also dissociated from the cell cortex and accumulate at the spindle poles in an astral microtubule– and LGN-dependent manner. The membrane localization of $G\alpha_i$ is mediated through cotranslational or posttranslational lipid modification (Chen and Manning, 2001) and, in principle, should not be affected by cortical actin filaments. We propose that

during mitosis, a large portion of $G\alpha_i$ is associated with LGN at the cell cortex in MDCK cells. Dynein-generated force could overcome the membrane attachment of $G\alpha_i$. Alternatively, other mitotic-specific mechanisms, such as depalmitoylation, may exist. In line with our hypothesis, a recent study in *C. elegans* revealed that the Gβ subunit GBP-1, a negative regulator of Gα/GPR1,2 complex, has the lowest membrane level during mitosis (Thyagarajan *et al.*, 2011). We are in the process of testing whether Gβ/γ and other $G\alpha_i$ regulators are involved in the transport of LGN/$G\alpha_i$.

The relationship between cortical actin filaments and dynein has long been an enigma. Previous studies suggest that actin filaments are required for the cortical localization of LGN and dynein subunits (Busson *et al.*, 1998; Kaushik *et al.*, 2003; Toyoshima *et al.*, 2007). Through careful analysis, we found that cortical dissociation of LGN and dynein upon disruption of actin filaments is not a simple event of anchorage detachment but involves astral MT–mediated transportation. We now provide a more definitive link between cortical actin filaments and the LGN/dynein complex. Our results suggest that actin filaments are not required for the cortical targeting of LGN/dynein; instead, they serve as a stabilizing structure to maintain the LGN/dynein complex at the cell cortex. We propose the existence of actin filament–associated or regulated protein(s) that links the LGN complex to cortical actin filaments and counteracts astral MT–mediated release of LGN/dynein complex. Such actin filament–mediated maintenance of cortical LGN/dynein may sustain dynein-generated forces or serve as a rate-limiting factor—by regulating the release and transport of the LGN/dynein complex—in modulating pulling forces on astral MTs under different physiological conditions.

Taking our results together, we propose the following working hypothesis (Figure 8C): membrane-associated Gα recruits LGN to the cell cortex, which in turn recruits NuMA and dynein. Cortical Gα/LGN/dynein/NuMA complex is stabilized and maintained by actin filaments through unknown factor(s). The interaction between astral MTs and the cell cortex is accompanied by constant release and transport of a portion of the Gα/LGN/dynein/NuMA complex from the cell cortex to spindle poles. Once reaching the spindle poles, the Gα/LGN/dynein/NuMA complex leaves the spindle poles and recycles back to the cell cortex. When dynein is knocked down or in the absence of astral MTs, the cortical release and transport of LGN will be compromised, and more LGN will be trapped at the cell cortex. On the other hand, when cortical actin filaments are disrupted, astral MTs mediate rapid release and transport of the Gα/LGN/dynein/NuMA complex, leading to its spindle pole accumulation. The cortical release, transport, and recycling of LGN is important for establishing the bipolar, symmetric cortical distribution of LGN during metaphase. The transport of LGN/dynein complex may also generate pulling forces on astral MTs or serve as a regulatory mechanism in balancing the pulling forces on astral MTs. Further studies are needed to elucidate how the dynamic behavior of cortical LGN complex is regulated at the molecular level and, of importance, to what extent the regulated transport of LGN/dynein complex contributes to spindle positioning.

MATERIALS AND METHODS

Cell lines and reagents

Cos 7 and MDCK cells were maintained in DMEM (Mediatech, Manassas, VA) supplemented with 10% fetal bovine serum and antibiotics at 37°C in a humidified 5% CO_2 atmosphere. Control, LGN-stable knockdown MDCK cell lines and Tet-Off MDCK cell line expressing Venus-LGN were described previously (Du and Macara, 2004; Zheng *et al.*, 2010).

Rabbit anti-LGN antibodies were described previously (Du and Macara, 2004). Rabbit anti-NuMA antibody was a kind gift from Duane Compton (Dartmouth Medical School, Hanover, NH). The following antibodies were also used: primary monoclonal 9E10 anti-myc, 12CA5 anti-hemagglutinin (HA; Santa Cruz Biotechnology, Santa Cruz, CA), anti-dynein (IC, DYNC1I1; clone 70.1; Sigma-Aldrich, St. Louis, MO), anti-$p150^{Glued}$ (Cell Signaling Technology, Danvers, MA), polyclonal rabbit anti-DYNC1H1, anti-$G\alpha_i3$ (Santa Cruz Biotechnology), and anti-GFP (Torry Pines Biolabs, Secaucus, NJ); secondary Alexa 488, Alexa 594, Alexa 660, and Alexa 680 (Invitrogen, Carlsbad, CA) and IRDye800-conjugated (Rockland Immuno-Chemicals, Gilbertsville, PA) goat anti-mouse or rabbit antibodies. Rhodamine–phalloidin was from Invitrogen; nocodazole, latrunculin A, monastrol, and MG132 were from Sigma-Aldrich.

Plasmids

Full-length human DYNC1H1 cDNA was transferred from KIAA cDNA clone (0325; Kazusa DNA Research Institute, Kisarazu, Japan) by PCR and restriction enzyme digestion and cloned in pK-VENUS (Du *et al.*, 2001). Human NuMAcDNA was PCR amplified and cloned into pKHA3 to generate pKHA3-NuMA. Wild-type $G\alpha_i1$ constructs were described previously (Du and Macara, 2004). Mutant $G\alpha_i1$ (N149I) was PCR amplified and cloned into pKmyc. For knocking down DYNC1H1 in MDCK cells, we used the pRNAi-neo plasmid (Biosettia, San Diego, CA) and the following target sequences: 5′-GCTGAAATCTGAAGCACTTAA-3′ (DYNC1H1 shRNA-1) and 5′-GCACTTAAAGATCGCCATTGG-3′ (DYNC1H1 shRNA-2).

Immunoprecipitation and Western blotting

Cos 7 cells were electroporated with mammalian expression vectors using an Amaxa Nucleofection device (Lonza, Basel, Switzerland) following the manufacturer's instructions. Cells were collected in lysis buffer (25 mM 4-(2-hydroxyethyl)-1-piperazineethanesulfonic acid [HEPES], pH 7.4, 150 mM NaCl, 0.5% Triton X-100, 0.5 mM EDTA, 5 mM $MgCl_2$, 1 mM dithiothreitol, 1 mM phenylmethylsulfonyl fluoride [PMSF], 10 μg/ml leupeptin, 20 μg/ml aprotinin, and 20 μg/ml pepstatin). Equal amounts of cell lysate were incubated with 2 μg of anti-myc, anti-HA, anti-LGN antibodies or rabbit IgG at 4°C for 2 h or overnight. GammaBind-Plus Sepharose beads (GE Healthcare, Pittsburgh, PA) were added, and the mixture was incubated for 1 h at 4°C. Beads were washed four times with cell lysis buffer, and bound proteins were separated by SDS–PAGE. Proteins were transferred to nitrocellulose membrane and detected using anti-myc (1:1000), anti-HA (1:2000), anti-LGN (1:500), anti-GFP (1:2000), anti-DYNC1H1 (1:200), anti-DYNC1I1 (1:1000), or anti-$p150^{Glued}$ (1:1000) antibodies.

Immunofluorescence microscopy

Cells were grown on poly-lysine–coated coverglass and fixed using either 4% paraformaldehyde (PFA) or 4% PFA/0.25% Triton X-100 in phosphate-buffered saline (PBS) as indicated. For detecting astral MT localization of LGN or cortical localization of DYNC1H1 and NuMA, cells were preextracted using PHEM buffer (25 mM HEPES, 60 mM 1,4-piperazinediethanesulfonic acid, 10 mM ethylene glycol tetraacetic acid, 2 mM $MgCl_2$, pH 6.9) containing 0.2% Triton X-100 and fixed in 4% PFA. Fixed cells were blocked with 1% bovine serum albumin/10% normal goat serum in PBS for 1 h and incubated in primary antibodies for 1 h at room temperature or overnight at 4°C. Cells were then washed and incubated for 1 h with the DNA dye Hoechst 33342 and secondary

antibodies coupled with Alexa 488 or Alexa 594 (Invitrogen). A SlowFade Gold AntiFade kit (Invitrogen) was used to reduce photobleaching. Cells were imaged using either a 60×/numerical aperture (NA) 1.2 oil-immersion objective on a Nikon TE2000 inverted microscope (Nikon Instruments, Melville, NY) or a 63×/NA 1.4 objective on a Zeiss 510 LSM confocal microscope (Carl Zeiss, Oberkochen, Germany).

Measurement of the relative fluorescence intensity of cortical and spindle pole LGN and $G\alpha_i3$ and of cortical NuMA and DYNC1H1

Measurements of the relative fluorescence intensity of cortical LGN or DYNC1H1 were performed as described (Wan *et al.*, 2012). Briefly, cells were stained with identical procedure, and images were taken with identical microscopic settings. Fifty metaphase cells in each group were randomly selected, and the mean fluorescence intensity of cortical LGN or DYNC1H1 was measured using ImageJ software (National Institutes of Health, Bethesda, MD). The standard deviation was calculated, and statistical significance was determined by Student's *t* test.

Similarly, for the measurement of the relative fluorescence intensity of spindle pole LGN, a 60-pixel circle was drawn around each spindle pole and in areas 10 pixels away using ImageJ software. Fluorescence intensities at the spindle poles and the cytosol were referred to as *F*(spindle pole) and *F*(cytosol), respectively. The ratio *F*(spindle pole)/*F*(cytosol) was collected for each group of cells and analyzed.

FRAP analysis

Stable Tet-Off MDCK cells expressing Venus-LGN were cultured in the absence (–Dox) of doxycycline to allow expression of low levels of Venus-LGN. Untreated cells or cells transfected with either control shRNA or DYNC1H1 shRNA were grown on Delta T dishes (Bioptechs, Butler, PA) in DMEM supplemented with 10% fetal calf serum (FCS) and antibiotics. At 1 h before FRAP analysis, the medium was replaced with F10 medium containing 10% FCS, and dimethyl sulfoxide (DMSO; 0.5%) or 50 nM nocodazole was added in the medium as needed. The dish was then placed in a temperature control system (Bioptechs) that maintained a temperature of 37°C during the FRAP experiment. FRAP experiments were performed on a LSM 7 live laser-scanning confocal microscope (Carl Zeiss) with a plan-Apochromat 63×/NA 1.4 oil objective. Because LGN accumulates at the cell cortex only during mitosis, it is easy to identify mitotic cells showing cortical Venus-LGN signal. We specifically chose those cortical areas where Venus-LGN fluorescence was relatively bright and smooth as the regions of interest (ROIs), which were 4 μm^2 in size and centered on the cortical Venus-LGN fluorescence. ROIs were first scanned with a 488-nm diode laser at 1.1% power for three cycles (10 s each cycle) to determine a measurement of initial fluorescence intensity in the ROI. Next ROIs were subjected to 12 iterations with 488-nm diode laser at 100% power to photobleach the ROI. The fluorescent images were then acquired every 10 s at 1.1% laser power for another 37 cycles using ZEN 2009 software (Carl Zeiss). The fluorescence recovery in the ROI at every time point was normalized according to $100(I_t - I_0)/(I_c - I_0)$, where I_t represents fluorescence intensity in the ROI at the given time point, I_0 represents the intensity of fluorescence in ROI after photobleaching, and I_c represents the average value of three measurements of the fluorescence intensity in the ROI before photobleaching. Recovery measurements were quantified by fitting normalized fluorescence intensities of bleached areas to a one-phase exponential association by using ZEN 2009 software (Carl Zeiss). Standard SEM was calculated, and statistical significance was determined by Student's *t* test.

ACKNOWLEDGMENTS

We thank Kazusa DNA Research Institute in Japan for kindly providing the KIAA clone. We are grateful to Duane Compton for providing the anti-NuMA antibody. This work was supported by grants from American Cancer Society (RSG0717601CSM) and the National Institutes of Health (GM079506) to Q.D.

REFERENCES

Adames NR, Cooper JA (2000). Microtubule interactions with the cell cortex causing nuclear movements in *Saccharomyces cerevisiae*. J Cell Biol 149, 863–874.

Ahringer J (2003). Control of cell polarity and mitotic spindle positioning in animal cells. Curr Opin Cell Biol 15, 73–81.

Ben-Yair R, Kahane N, Kalcheim C (2011). LGN-dependent orientation of cell divisions in the dermomyotome controls lineage segregation into muscle and dermis. Development 138, 4155–4166.

Bowman SK, Neumuller RA, Novatchkova M, Du Q, Knoblich JA (2006). The *Drosophila* NuMA homolog Mud regulates spindle orientation in asymmetric cell division. Dev Cell 10, 731–742.

Busson S, Dujardin D, Moreau A, Dompierre J, De Mey JR (1998). Dynein and dynactin are localized to astral microtubules and at cortical sites in mitotic epithelial cells. Curr Biol 8, 541–544.

Carminati JL, Stearns T (1997). Microtubules orient the mitotic spindle in yeast through dynein-dependent interactions with the cell cortex. J Cell Biol 138, 629–641.

Chen CA, Manning DR (2001). Regulation of G proteins by covalent modification. Oncogene 20, 1643–1652.

Chia W, Somers WG, Wang H (2008). *Drosophila* neuroblast asymmetric divisions: cell cycle regulators, asymmetric protein localization, and tumorigenesis. J Cell Biol 180, 267–272.

Collins ES, Balchand SK, Faraci JL, Wadsworth P, Lee WL (2012). Cell cycle-regulated cortical dynein/dynactin promotes symmetric cell division by differential pole motion in anaphase. Mol Biol Cell 23, 3380–3390.

Colombo K, Grill SW, Kimple RJ, Willard FS, Siderovski DP, Gonczy P (2003). Translation of polarity cues into asymmetric spindle positioning in *Caenorhabditis elegans* embryos. Science 300, 1957–1961.

Couwenbergs C, Labbe JC, Goulding M, Marty T, Bowerman B, Gotta M (2007). Heterotrimeric G protein signaling functions with dynein to promote spindle positioning in *C. elegans*. J Cell Biol 179, 15–22.

Dujardin DL, Vallee RB (2002). Dynein at the cortex. Curr Opin Cell Biol 14, 44–49.

Du Q, Macara IG (2004). Mammalian Pins is a conformational switch that links NuMA to heterotrimeric G proteins. Cell 119, 503–516.

Du Q, Stukenberg PT, Macara IG (2001). A mammalian Partner of Inscuteable binds NuMA and regulates mitotic spindle organization. Nat Cell Biol 3, 1069–1075.

Du Q, Taylor L, Compton DA, Macara IG (2002). LGN blocks the ability of NuMA to bind and stabilize microtubules. A mechanism for mitotic spindle assembly regulation. Curr Biol 12, 1928–1933.

El-Hashash AH, Turcatel G, Al Alam D, Buckley S, Tokumitsu H, Bellusci S, Warburton D (2011). Eya1 controls cell polarity, spindle orientation, cell fate and Notch signaling in distal embryonic lung epithelium. Development 138, 1395–1407.

El-Hashash AH, Warburton D (2011). Cell polarity and spindle orientation in the distal epithelium of embryonic lung. Dev Dynam 240, 441–445.

Faulkner NE, Dujardin DL, Tai CY, Vaughan KT, O'Connell CB, Wang Y, Vallee RB (2000). A role for the lissencephaly gene LIS1 in mitosis and cytoplasmic dynein function. Nat Cell Biol 2, 784–791.

Fink J *et al.* (2011). External forces control mitotic spindle positioning. Nat Cell Biol 13, 771-U401.

Fuse N, Hisata K, Katzen AL, Matsuzaki F (2003). Heterotrimeric G proteins regulate daughter cell size asymmetry in *Drosophila* neuroblast divisions. Curr Biol 13, 947–954.

Gaetz J, Kapoor TM (2004). Dynein/dynactin regulate metaphase spindle length by targeting depolymerizing activities to spindle poles. J Cell Biol 166, 465–471.

Gillies TE, Cabernard C (2011). Cell division orientation in animals. Curr Biol 21, R599–R609.
Gonczy P (2008). Mechanisms of asymmetric cell division: flies and worms pave the way. Nat Rev Mol Cell Biol 9, 355–366.
Gotta M, Ahringer J (2001). Distinct roles for Galpha and Gbetagamma in regulating spindle position and orientation in *Caenorhabditis elegans* embryos. Nat Cell Biol 3, 297–300.
Gotta M, Dong Y, Peterson YK, Lanier SM, Ahringer J (2003). Asymmetrically distributed *C. elegans* homologs of AGS3/PINS control spindle position in the early embryo. Curr Biol 13, 1029–1037.
Grill SW, Gonczy P, Stelzer EH, Hyman AA (2001). Polarity controls forces governing asymmetric spindle positioning in the *Caenorhabditis elegans* embryo. Nature 409, 630–633.
Grill SW, Howard J, Schaffer E, Stelzer EH, Hyman AA (2003). The distribution of active force generators controls mitotic spindle position. Science 301, 518–521.
Grill SW, Hyman AA (2005). Spindle positioning by cortical pulling forces. Dev Cell 8, 461–465.
Hao Y, Du QS, Chen XY, Zheng Z, Balsbaugh JL, Maitra S, Shabanowitz J, Hunt DF, Macara IG (2010). Par3 controls epithelial spindle orientation by aPKC-mediated phosphorylation of apical pins. Curr Biol 20, 1809–1818.
Hendricks AG, Lazarus JE, Perlson E, Gardner MK, Odde DJ, Goldman YE, Holzbaur ELF (2012). Dynein tethers and stabilizes dynamic microtubule plus ends. Curr Biol 22, 632–637.
Izumi Y, Ohta N, Hisata K, Raabe T, Matsuzaki F (2006). *Drosophila* Pins-binding protein Mud regulates spindle-polarity coupling and centrosome organization. Nat Cell Biol 8, 586–593.
Jordan MA, Thrower D, Wilson L (1992). Effects of vinblastine, podophyllotoxin and nocodazole on mitotic spindles. Implications for the role of microtubule dynamics in mitosis. J Cell Sci 102, 401–416.
Kardon JR, Vale RD (2009). Regulators of the cytoplasmic dynein motor. Nat Rev Mol Cell Biol 10, 854–865.
Kaushik R, Yu F, Chia W, Yang X, Bahri S (2003). Subcellular localization of LGN during mitosis: evidence for its cortical localization in mitotic cell culture systems and its requirement for normal cell cycle progression. Mol Biol Cell 14, 3144–3155.
Kimura K, Kimura A (2011). Intracellular organelles mediate cytoplasmic pulling force for centrosome centration in the *Caenorhabditis elegans* early embryo. Proc Natl Acad Sci USA 108, 137–142.
Kisselev AF, Goldberg AL (2001). Proteasome inhibitors: from research tools to drug candidates. Chem Biol 8, 739–758.
Kisurina-Evgenieva O, Mack G, Du Q, Macara I, Khodjakov A, Compton DA (2004). Multiple mechanisms regulate NuMA dynamics at spindle poles. J Cell Sci 117, 6391–6400.
Kiyomitsu T, Cheeseman IM (2012). Chromosome- and spindle-pole-derived signals generate an intrinsic code for spindle position and orientation. Nat Cell Biol 14, 311–317.
Knoblich JA (2008). Mechanisms of asymmetric stem cell division. Cell 132, 583–597.
Konno D, Shioi G, Shitamukai A, Mori A, Kiyonari H, Miyata T, Matsuzaki F (2008). Neuroepithelial progenitors undergo LGN-dependent planar divisions to maintain self-renewability during mammalian neurogenesis. Nat Cell Biol 10, 93–101.
Kotak S, Busso C, Gonczy P (2012). Cortical dynein is critical for proper spindle positioning in human cells. J Cell Biol 199, 97–110.
Kunda P, Baum B (2009). The actin cytoskeleton in spindle assembly and positioning. Trends Cell Biol 19, 174–179.
Laan L, Pavin N, Husson J, Romet-Lemonne G, van Duijn M, Lopez MP, Vale RD, Julicher F, Reck-Peterson SL, Dogterom M (2012). Cortical dynein controls microtubule dynamics to generate pulling forces that position microtubule asters. Cell 148, 502–514.
Lanier SM (2004). AGS proteins, GPR motifs and the signals processed by heterotrimeric G proteins. Biol Cell 96, 369–372.
Matsumura S, Hamasaki M, Yamamoto T, Ebisuya M, Sato M, Nishida E, Toyoshima F (2012). ABL1 regulates spindle orientation in adherent cells and mammalian skin. Nat Commun 3, 626.
Mayer TU, Kapoor TM, Haggarty SJ, King RW, Schreiber SL, Mitchison TJ (1999). Small molecule inhibitor of mitotic spindle bipolarity identified in a phenotype-based screen. Science 286, 971–974.
McCarthy EK, Goldstein B (2006). Asymmetric spindle positioning. Curr Opin Cell Biol 18, 79–85.
Merdes A, Ramyar K, Vechio JD, Cleveland DW (1996). A complex of NuMA and cytoplasmic dynein is essential for mitotic spindle assembly. Cell 87, 447–458.
Morin X, Bellaiche Y (2011). Mitotic spindle orientation in asymmetric and symmetric cell divisions during animal development. Dev Cell 21, 102–119.
Morin X, Jaouen F, Durbec P (2007). Control of planar divisions by the G-protein regulator LGN maintains progenitors in the chick neuroepithelium. Nat Neurosci 10, 1440–1448.
Nguyen-Ngoc T, Afshar K, Gonczy P (2007). Coupling of cortical dynein and G alpha proteins mediates spindle positioning in *Caenorhabditis elegans*. Nat Cell Biol 9, 1294–1302.
Nipper RW, Siller KH, Smith NR, Doe CQ, Prehoda KE (2007). Galphai generates multiple Pins activation states to link cortical polarity and spindle orientation in *Drosophila* neuroblasts. Proc Natl Acad Sci USA 104, 14306–14311.
O'Connell CB, Wang YL (2000). Mammalian spindle orientation and position respond to changes in cell shape in a dynein-dependent fashion. Mol Biol Cell 11, 1765–1774.
Parmentier ML, Woods D, Greig S, Phan PG, Radovic A, Bryant P, O'Kane CJ (2000). Rapsynoid/partner of inscuteable controls asymmetric division of larval neuroblasts in *Drosophila*. J Neurosci 20, RC84.
Pecreaux J, Roper JC, Kruse K, Julicher F, Hyman AA, Grill SW, Howard J (2006). Spindle oscillations during asymmetric cell division require a threshold number of active cortical force generators. Curr Biol 16, 2111–2122.
Peyre E, Jaouen F, Saadaoui M, Haren L, Merdes A, Durbec P, Morin X (2011). A lateral belt of cortical LGN and NuMA guides mitotic spindle movements and planar division in neuroepithelial cells. J Cell Biol 193, 141–154.
Poulson ND, Lechler T (2010). Robust control of mitotic spindle orientation in the developing epidermis. J Cell Biol 191, 915–922.
Sachdev P, Menon S, Kastner DB, Chuang JZ, Yeh TY, Conde C, Caceres A, Sung CH, Sakmar TP (2007). G protein beta gamma subunit interaction with the dynein light-chain component Tctex-1 regulates neurite outgrowth. EMBO J 26, 2621–2632.
Samora CP, Mogessie B, Conway L, Ross JL, Straube A, McAinsh AD (2011). MAP4 and CLASP1 operate as a safety mechanism to maintain a stable spindle position in mitosis. Nat Cell Biol 13, U1040–U1059.
Schaefer M, Petronczki M, Dorner D, Forte M, Knoblich JA (2001). Heterotrimeric G proteins direct two modes of asymmetric cell division in the *Drosophila* nervous system. Cell 107, 183–194.
Schaefer M, Shevchenko A, Shevchenko A, Knoblich JA (2000). A protein complex containing Inscuteable and the Galpha-binding protein Pins orients asymmetric cell divisions in *Drosophila*. Curr Biol 10, 353–362.
Siller KH, Cabernard C, Doe CQ (2006). The NuMA-related Mud protein binds Pins and regulates spindle orientation in *Drosophila* neuroblasts. Nat Cell Biol 8, 594–600.
Siller KH, Doe CQ (2009). Spindle orientation during asymmetric cell division. Nat Cell Biol 11, 365–374.
Spector I, Shochet NR, Kashman Y, Groweiss A (1983). Latrunculins: novel marine toxins that disrupt microfilament organization in cultured cells. Science 219, 493–495.
Srinivasan DG, Fisk RM, Xu H, van den Heuvel S (2003). A complex of LIN-5 and GPR proteins regulates G protein signaling and spindle function in *C. elegans*. Genes Dev 17, 1225–1239.
Thery M, Racine V, Pepin A, Piel M, Chen Y, Sibarita JB, Bornens M (2005). The extracellular matrix guides the orientation of the cell division axis. Nat Cell Biol 7, 947–953.
Thyagarajan K, Afshar K, Gonczy P (2011). Polarity mediates asymmetric trafficking of the G beta heterotrimeric G-protein subunit GPB-1 in *C. elegans* embryos. Development 138, 2773–2782.
Toyoshima F, Matsumura S, Morimoto H, Mitsushima M, Nishida E (2007). PtdIns(3,4,5)P3 regulates spindle orientation in adherent cells. Dev Cell 13, 796–811.
Toyoshima F, Nishida E (2007). Integrin-mediated adhesion orients the spindle parallel to the substratum in an EB1- and myosin X-dependent manner. EMBO J 26, 1487–1498.
van der Voet M, Berends CW, Perreault A, Nguyen-Ngoc T, Gonczy P, Vidal M, Boxem M, van den Heuvel S (2009). NuMA-related LIN-5, ASPM-1, calmodulin and dynein promote meiotic spindle rotation independently of cortical LIN-5/GPR/Galpha. Nat Cell Biol 11, 269–277.
Wan QW, Liu J, Zheng Z, Zhu HB, Chu XG, Dong Z, Huang S, Du QS (2012). Regulation of myosin activation during cell-cell contact formation by Par3-Lgl antagonism: entosis without matrix detachment. Mol Biol Cell 23, 2076–2091.

Werts AD, Roh-Johnson M, Goldstein B (2011). Dynamic localization of C. elegans TPR-GoLoco proteins mediates mitotic spindle orientation by extrinsic signaling. Development 138, 4411–4422.
Willard FS *et al.* (2008). A point mutation to Galphai selectively blocks GoLoco motif binding: direct evidence for Galpha. GoLoco complexes in mitotic spindle dynamics. J Biol Chem 283, 36698–36710.
Willard FS, Kimple RJ, Siderovski DP (2004). Return of the GDI: the GoLoco motif in cell division. Annu Rev Biochem 73, 925–951.
Williams SE, Beronja S, Pasolli HA, Fuchs E (2011). Asymmetric cell divisions promote Notch-dependent epidermal differentiation. Nature 470, 353–358.
Woodard GE, Huang NN, Cho H, Miki T, Tall GG, Kehrl JH (2010). Ric-8A and Gi alpha recruit LGN, NuMA, and dynein to the cell cortex to help orient the mitotic spindle. Mol Cell Biol 30, 3519–3530.
Xiao ZN, Wan QW, Du QS, Zheng Z (2012). Galpha/LGN-mediated asymmetric spindle positioning does not lead to unequal cleavage of the mother cell in 3-D cultured MDCK cells. Biochem Biophys Res Commun 420, 888–894.
Yu F, Kuo CT, Jan YN (2006). *Drosophila* neuroblast asymmetric cell division: recent advances and implications for stem cell biology. Neuron 51, 13–20.
Zheng Z, Zhu HB, Wan QW, Liu J, Xiao ZN, Siderovski DP, Du QS (2010). LGN regulates mitotic spindle orientation during epithelial morphogenesis. J Cell Biol 189, 275–288.
Zhu JW, Wen WY, Zheng Z, Shang Y, Wei ZY, Xiao ZN, Pan Z, Du QS, Wang WN, Zhang MJ (2011). LGN/mInsc and LGN/NuMA complex structures suggest distinct functions in asymmetric cell division for the Par3/mInsc/LGN and G alpha i/LGN/NuMA pathways. Mol Cell 43, 418–431.